Desalination and Water Treatment
www.deswater.com

doi: 10.5004/dwt.2023.30058

315 (2023) 13–23
December

Study for mechanical vapor compression desalination carried out at ambient pressure in several concentration steps which shows a very high efficiency thanks to a specific condensing pipe/chamber and a heat exchanger with fluids in laminar flow

Mario Vismara

Via Lavoro 5, 23880 Casatenovo (LC), Italy, email: mariovisma@tiscali.it

Received 20 July 2023; Accepted 14 October 2023

ABSTRACT

Current mechanical vapor compression (MVC) technology has almost completely lost interest in the desalination market; MVC is affected by the complication of the system, the high cost of the plant and the unacceptable electric power demand, factors which cannot be compensated by a better quality of the water produced, by less need for treatment of the fluids and by a much better profile under the aspect of safety control and potential induced pollution. Since the energy requirement of the current MVC technique, as described in literature, is not justified in thermodynamic terms, the study analyzes the problems and illustrates a possible solution resorting to multiple concentration steps with operation at ambient pressure, with a particular condensing chamber and an aluminum heat exchanger with flux of fluids in laminar motion. Assuming a mechanical efficiency of 75%, an electrical efficiency of 94% and a cost of electricity of 0.1 $/kWh, the optimal value of electrical energy required for desalination from 35 to 70 ppt obtained in the study is 3.0 kWh/ton.

Keywords: Laminar motion heat exchanger; Mechanical vapor compression; $CaCO_3$ scaling

1. Introduction

This article is a further development of a search for solutions aiming to bring mechanical vapor compression (MVC) to economic competitiveness. The project was named GMVC where G stands for Green as the project aims to reduce energy demands. The first approach using plastic has been the subject of an article published by the author in July 2021 [1]. Subsequently, having identified the heat exchanger (HX) connected to the MVC plant as critical to reach a positive result, a research was carried out to study HXs operating in laminar motion showing high energy efficiency and low economic costs. A first study on a plastic solution, with particular attention to Computational Fluid Dynamics (CFD) calculations was carried out at the Politecnico of Milan, published in 2023 [2]. This is a third article intended to illustrate the thermodynamic results theoretically achievable with a GMVC variant of the MVC which resorts to aluminum instead of plastic as interface for the heat exchanges both in the evaporator/condenser and in HX components.

The choice of aluminum was made to faciltate the study to be carried out. It does not constitute a limitation. The study is fundamentally open to the use of its alloys (in particular the 5052 aluminum alloy which is particularly resistant to corrosion in the presence of salts and high temperatures) and of other metals and their alloys should a higher resistance to corrosion be needed; in this case, because of higher costs this may lead to an increase in the optimum ΔT for heat transfer.

With reference to desalination powered exclusively by electricity, reverse osmosis has almost completely replaced MVC technology. MVC has in fact suffered from the extreme complication of the system, for its high cost and for unacceptably high electricity consumption [3], factors that could not be compensated for by better quality of the water produced, less need for pre-treatment of fluids and by a clearly better profile in terms of potential induced pollution, not even today despite increasing attention to the ecological impact of desalination plants which is beginning to impose itself for the technical requirements for new plants.

Our new GMVC study intends to carry out a radical revision of the MVC process and to reduce both the high electrical energy demand and investment costs:

- Referring to the costs of the plant the research assumes the need to operate at ambient pressure and therefore at approx. 100°C, unlike what happens in the known MVC process which normally operates at 60°C and therefore at a pressure lower than the atmospheric one. The reasons which had led the former MVC solution to opt for low pressure were mainly the high request of energy by the heat exchanger and a lower solubility of $CaCO_3$. A new MVC solution which solves these issues would allow a series of very important advantages. These are:

(a) Avoiding the need for expensive pressure resistant containers which are necessarily made of metal and place constraints on the volumes available. Operating at ambient pressure, the insulated container within which condensation and evaporation occurs could have an almost negligible cost.
(b) Vacuum pumps are no longer required.
(c) There are practically no restrictions on the size of the container and its accessibility inside: this favors inspection, cleaning and maintenance.
(d) Availability of low-cost space favors the organization of the condensation chambers in packs on a number of removable blocks that provide the possibility of centralized filling and purging and to carry out the distillation in several concentration steps as well as allowing modularity.
(e) It allows operating evaporation with large flat evaporative surfaces, so no need of spraying. Evaporation requires only small ΔT over boiling-point elevation (BPE) and can take place in the absence of boiling: there are no droplets of salt water in the produced steam and therefore no need of demisters and there is no contact of salt water with the walls of the container; the water produced is very pure and free from carryover.

- Referring to the high energy demand the considerations which led to conceive the GMVC process consist above all in the fact that the energy demand of the current MVC technique, as described in literature, is not justified in thermodynamic terms: for example, MVC desalination of a 70 ppt water salinity, at 100°C, under ideal thermodynamic conditions would require only 1.8 kWh/ton.

With regard to energy consumption, we have found several advantages that can be obtained:

(a) The organization of the condensation chambers in a number of removable blocks allows the evaporative process to be performed in multiple steps. Taking advantage of the lower energy requirements of the initial concentration steps consistently improves the overall efficiency of the process.
(b) Operating with a large evaporative surface can reduce the ΔT for heat transfer and so allows for energy savings: the proposed structure is composed of thin chambers close together, arranged vertically with evaporation occurring on both sides: the heat exchange surfaces per volume unit are huge.
(c) Feeding of saline water carried out in discontinuous mode allows to reduce the thickness of the percolating saline solution and to increase the overall heat exchange and productivity.

- With reference the heat exchanger component, we observed that the thermal energy available to make up for the HX needs should exclusively be the one originating from the transformation into heat of the electrical energy used for compression. This means that to achieve the goal of a very efficient evaporation–condensation, that is, a lower energy required for compression, a very high efficiency of the HX is essential.

Unfortunately, the HXs available at affordable costs are not able to support a very efficient MVC evaporator/condenser: the most efficient HXs are not only a very expensive investment, but imply high energy demands for fluid pumping since they resort to an increasingly turbulent motion of fluids which requires high pumping energies.

The need to find a compromise between the HX and evaporator/condenser efficiencies largely explains the limits shown by the current MVC technology. In conclusion, with reference to energy consumption, the HX represents the most critical part of a MVC upgrade and the search for a possible solution has been the main task of our study.

2. Laminar motion HX for a green MVC

In order to have a HX suitable for the needs of GMVC we have studied a particular version which operates in laminar motion, so with minimal pumping energy requests. A first plastic version studied, with particular reference to the CFD calculations made by the Politecnico University of Milan, was the subject of an earlier publication [2].

The CFD study made it possible to find correlations which facilitate the calculation of heat exchange values that can be reached when flows a few tenths of a millimeter thick moving in laminar motion are split by an adiabatic wall. According to those correlations it was therefore possible to evaluate also an aluminum version of the HX we designed. The results confirmed the possibility of satisfying, with low economic costs and an high energy performance, the HX's efficiency requests that occur when the compression/condensation phase of MVC is closer to the thermodynamic theoretical values.

The study of the aluminum HX required to find a satisfactory solution to problems that arise under various aspects, such as, for example, the difficulty of feeding two counter flows between large but very closely spaced plates maintaining a sufficient uniformity of the motion of the fluid along its path, the need to avoid deformation of the aluminum sheet in the presence of variable fluid pressures in different positions of the HX, the need to be able to deal with fouling/sedimentation problems without compromising the homogeneity of the flows, that of making it possible to eliminate the non-condensable gas (NCGs) dissolved in the feed water that the increase in temperature had promoted to the gaseous state.

The solution we found solves these problems and offers additional benefits. It is based on the design of a particular slab in molded plastic and on the interposition of the same between the aluminum sheets which preside over the heat exchanges. This plastic slab performs numerous functions although it does not have direct heat exchange functions as it is in a permanent adiabatic state. However, by dividing each counterflow into two parts mirroring each other, its presence contributes substantially to the improvement of heat exchanges as it slows down the flow in the layer of fluid farthest from the heat exchange surfaces. When operating in laminar motion the correlation found thanks to the CFD study allows, introducing a coefficient, to use the classical simple formula used for calculating thermal conduction in a series of flat solid materials:

$$Q = \frac{\Delta T}{\left(y_1 / k_{1a} + y_2 / k_{2a} + y_3 / k_{3a}\right)} \tag{1}$$

where y_1 is the thickness of the flux, y_2 is the thickness of the aluminum foil, y_3 is the thickness of the counterflow, k_1, k_2 and k_3 are the thermal conductivities of the two fluids and aluminum, y_1, y_2, y_3 represent the relative thicknesses and ΔT the temperature differential); using the LMDT value (logarithmic mean temperature difference between the two flows) as ΔT in the formula, the values calculated with CFD correspond to those calculated with the above formula by multiplying the thickness of the flows by a coefficient of 0.36. To give a practical example, assuming a fluid thickness of 0.2 mm (with an average water thermal conductivity in the temperature range 20°C–90°C of 0.63 W/m·°C) and an aluminum foil thickness of 0.5 mm (thermal conductivity 204 W/m·°C), we obtain a thermal power value of approx. 4.33 kW/(m^2·°C); assuming that the adiabatic slab has a thickness of 4 mm and that the useful heat exchange surface is equal to 80% of its surface, we therefore obtain per unit volume of a block made of overlapping slabs and aluminum sheets a thermal power of about 865 kW/(m^3·°C).

Our HX solution has other advantages such as: (a) it allows the construction of blocks of considerable size, modular both in size and in number as they can be arranged in parallel; (b) the large sections for the passage of fluids obtainable (e.g., about 800 cm^2/m^2 of the block section as in the example given above) allow to limit both the length of the fluid path and its speed, factors which both allow to reduce pressure drop and so pumping energy needs. For example, for a flow thickness of 0.2 mm and an average fluid speed of 286 m/h, the CFD calculations mentioned show a pressure drop of 0.134 kg/cm^2 per linear meter; that means that for a preferred length of 1.7 m pumping energy consumption is almost irrelevant: an excellent result considering that one of the goals of the research we did on the HX was precisely to lower the electrical cost of pumping; (c) the limited useful length allows the HX to be arranged vertically allowing for better management in case of a possible creation of sediments and/or the need to purge undesirable NCG.

The slab we studied, illustrated in Fig. 1, also has the following specifics:

(1) They can be superimposed in large numbers, therefore a high modularity and the achievement of high fluid passage sections for each block/pack is allowed.
(2) The slabs are dotted with numerous thin protuberances that have the function of providing support to the aluminum sheets so that they can resist both the pressure differentials between the counterflows and the external pressure which is applied to the block of overlapping layers to keep them united and compact. These protuberances have a profile so as to interfere as little as possible with the flow of fluids.
(3) The slab's surface is also provided with numerous through holes which ensure the uniform distribution of the fluid, especially in the event of the formation of deposits (sediments and/or incrustations).
(4) Vertical through incisions are present in the outer edge which serve to house the profiles that will constitute the flow and outflow channels of the liquids in a watertight manner.

3. Evaporator/condenser structure

As known, the MVC technology involves feeding the preheated water to be distilled into a container filled with vapor where it is brought into contact with hot pipes, so as to make it partially evaporate. The steam produced is then compressed and introduced inside said pipes. Pipes constitute a so-called "condensation chamber" since inside them, in consideration of the pressure applied to the steam, it precisely condenses and the thermal energy connected to the condensation is transmitted by conduction to the external side of the pipes, supplying them with the heat necessary to promote evaporation.

The efficiency of the evaporation/condensation process is evidently greater the more efficient are the heat exchanges that take place between the saline aqueous layer that wets the pipes, the metal layer that makes up the pipe and the water layer that condenses inside the pipes. Other conditions (such as the salinity of the water supplied, the applied pressure differential, the evaporation surface and the thermal conductivity of the material with which the pipe is produced) being equal, the entity of the heat exchanges will be greater the lower the resistance to thermal conduction of these layers, that is, the thinner the layer of saline water, that of the distilled water which condenses and the one of the pipe.

Taking these elements into account, we can observe:

(a) In consideration of the very high conductivity of the metals that make up the pipes (e.g., aluminum has a conductivity of 204 W/m·°C compared to that of water of 0.63 W/m·°C), the resistance to thermal conductivity represented by this layer is not very relevant.
(b) As for the external layer of saline water that wets the pipe, optimization is achieved by feeding the saline water in an intermittent/discontinuous mode, that is, letting most of the water fed onto the surface of the pipe initially percolate, leaving, after a very short time,

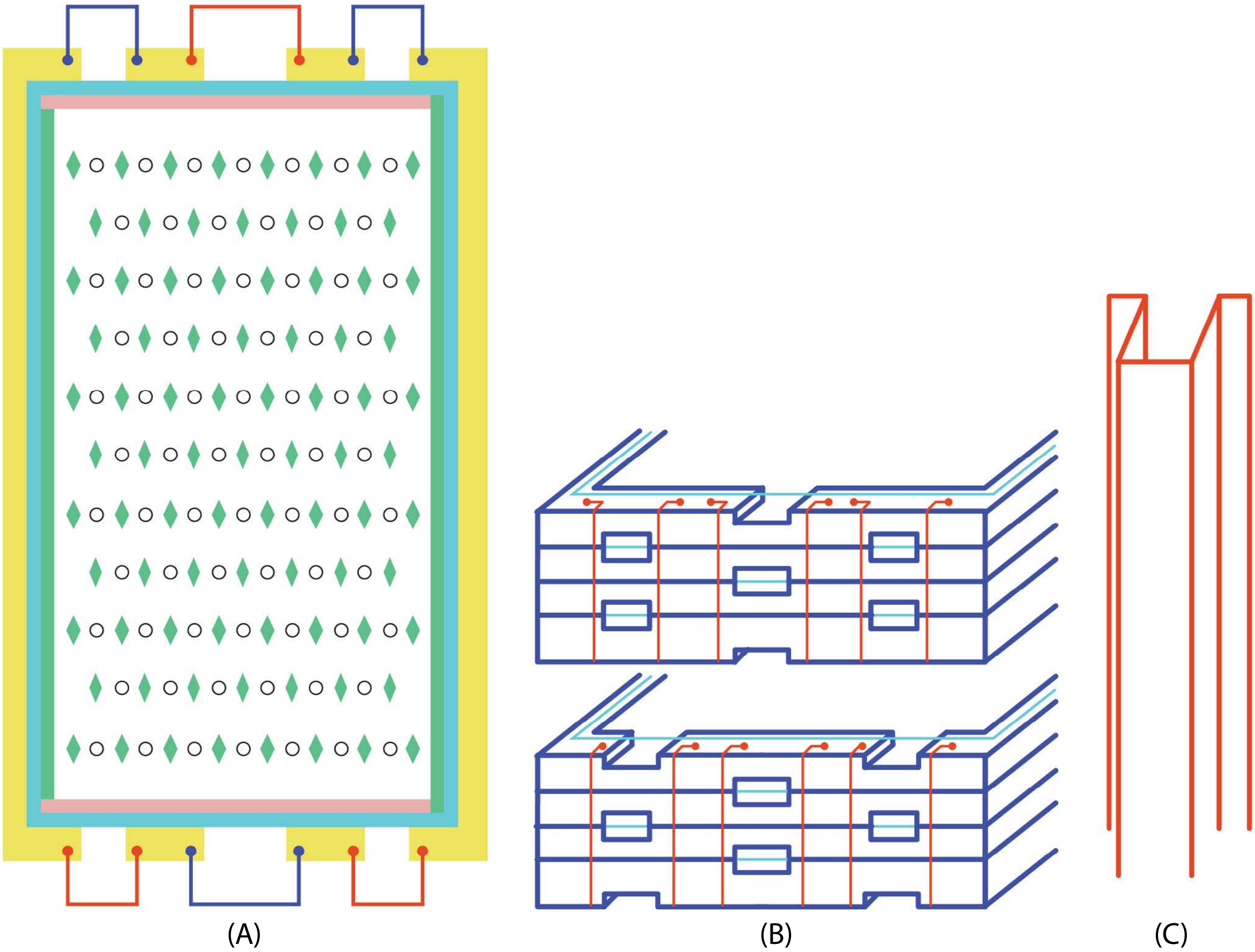

Fig. 1. (A) Plan view of a slab: the blue color indicates the edges of the aluminum sheet, the green color indicates the protuberances and lateral support points on the aluminum sheet, the small circles are the through holes to homogenize the upper flows and protect against possible deposits; on the sides in blue and red the profiles that make up the supply and purge channels for each of the two counterflows, (B) two side views of a portion of a block, and (C) profile that forms the flow and outflow channels.

a very thin layer which then partially evaporates and becomes even thinner. With this optimization the conductivity in the external layer is very high.

(c) As for the inner layer, the condensation is continuous and feeds a small layer which, as it is percolating, tends to thicken and, while not reaching particularly high thickness, nonetheless constitutes an important and often the main global resistance to heat exchanges in the evaporator/condenser.

In order to find improvements to the previous technology using aluminum pipes, various possibilities have been analyzed to obtain greater efficiency both in the arrangement of the constituent elements and in improving the conductivity of the various layers by modifying the structure of the pipes.

With reference to the outer layer, we have observed that if the intermittent/discontinuous feeding was performed on a vertical flat surface instead of on pipes, some advantages would be gained: (i) a more uniform and thinner thickness of the liquid on the surface; (ii) a greater ease of feeding of the liquid, avoiding splashes which cause droplets which are dispersed in the vapor and then require the presence of demisters to avoid both the pollution of the condensate and damages on the compressors; (iii) easier cleaning and removal of any incrustations that may form. On the other hand, the pipes ensure an excellent and necessary guide of the steam from the supply side to the opposite one, where purges must be carried out to eliminate NCG.

We therefore looked for a solution that could combine the advantages presented by the tube and those presented by the flat evaporative surface. The solution we have found consists in resorting to a condensation chamber made up of extruded tubular elements with a particular elongated profile as illustrated in Fig. 2A and B resulting in a condensation chamber which therefore constitutes a hybrid between the condensing chamber with tubes and the one made with flat plates.

Fig. 2B and C show the profiles of what we called "hybrid tubes". These components can be obtained by aluminum

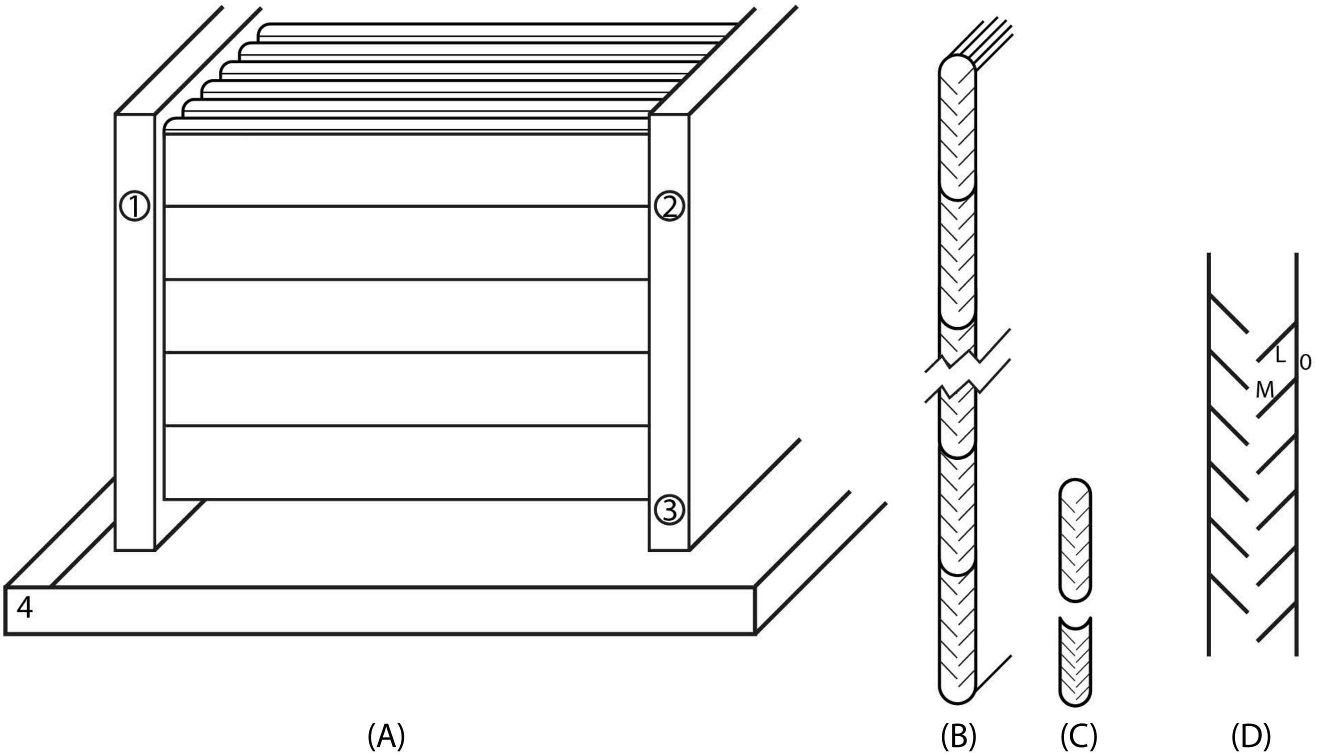

Fig. 2. (A) Set-up of the evaporator block which includes two heads to which "hybrid tubes" are connected: (I) vapor inlet; (II) purging of non-condensable gases; (III) purging of the water produced by the condensed steam; (IV) collection tank for percolated water. (B,C) Set-up of hybrid pipes, and (D) thermal connection of the "L" and "M" fins with the "O" portion of the hybrid tube wall.

extrusion and show a tubular profile with elongated flat external walls while on the inner side they have inclined fins which have various important functions. These "hybrid tubes" can be very thin: in the case of not particularly long tubes, their width can be around 1 cm. Furthermore, the overlapping of several "hybrid tubes" (Fig. 2C) allows the creation of heat exchange surfaces of large dimensions in which the external surface appears as a substantially flat surface.

The "hybrid tubes" thus conceived, thanks to the fins, protuberances coextruded in contact with the external wall of the tube as highlighted in Fig. 2B and C and with the letters L and M in Fig. 2D, perform a triple beneficial action for the efficiency of the device:

(1) The presence of the inclined fins avoids a thickening of the percolating condensed water which they discharge to the center of the "hybrid pipe"; the drainage thus obtained substantially improves the efficiency of heat exchanges.
(2) The fins allow an orderly movement of the steam from the supply side to the opposite one, where a partial purge of the steam takes place; in fact, following progressive condensation of steam along the way, its content of NCG progressively increases until it hinders condensation and makes bleeding necessary. The guiding effect of the fins makes it possible to avoid mixing and limits the negative effect/impact due to NCG on condensation to the last section of the "pipes" and also it reduces the extent of the purges.
(3) In consideration of the high conductivity of aluminum the fins are able to exchange considerable quantities of heat with the external wall of the "hybrid pipe" in contact with the saline liquid to be evaporated; as illustrated schematically in Fig. 2D the walls of the fins marked with L and M participate in the condensation of vapor and the relative heat of condensation adds to the one that occurs on the wall "O".

Considering that the thickness of the percolating layer after about 1 s from the discontinuous supply assumes a value of approx. 0.035 mm and that the condensing layer, taking into account the contribution to heat exchanges provided by the fins, assumes an "equivalent" thickness which we have estimated at approx. 0.025 mm, the heat exchange value per m^2 of surface is extremely high, reaching a value of about 10.000 W/m^2·°C (Table 2).

4. Optimal ΔT for heat transfer in evaporator/condenser

Improvements in heat transfer are invaluable in both, increasing production and reducing the ΔT for heat transfer, that is, energy requirements; the choice of the most economically advantageous way to pursue is usually made by searching for the optimal ΔT for heat exchange for the plant.

The economic efficiency of desalination per ton of water produced depends on multiple parameters that contribute and interact. Among these the main ones are: the salinity of the supply and the concentration carried out, the possibility of operating in several steps of concentration, the cost of electricity, the relative average hourly production of the plant, the capital recovery rate of investment per ton of distilled water produced (which is a function of both its cost and its expected life, of a possible residual value when decommissioned and of the interest rate which exceeds inflation), the vapor compression pressure, the electrical and mechanics efficiency of pumps and compressors, heat losses, HX efficiency, etc.

For some of these parameters, with reference to the process we studied, we can observe:

- In relation to the energy for pumping the fluids, considering the low pressure drop in the HX highlighted above, these costs are not very significant and overall, for HX and evaporator/condenser, they result from our calculations of approx. 0.15 kWh/ton of distillate.
- In relation to the compression thermodynamic energy demand, which is proportional to the entity of the BPE, as shown in Table 1, it is possible to observe important savings by operating in several concentration steps: for example, operating in 5 ppt concentration steps from 35 to 70 ppt the weighted average BPE value is only approx. 0.8°C compared to the value of 1.14°C achieved in the final step at 70 ppt; the multi-step operation made easy by our project therefore allows a saving in the BPE value of approx. 0.34°C, or 30% approx. of the thermodynamic energy demand, compared to what happens in the technique that operates in a single step.
- In relation to the overall energy demand of the compression it is advisable to evaluate the most advantageous or "optimal" ΔT for heat transfer, ΔT which added to the thermodynamic ΔT will characterize the compression.

The calculation of the "optimal ΔT for heat transfer" depends significantly on economic factors such as the cost of electricity and the capital recovery rate of the cost of the plant per ton/h produced. With regards to the plant's cost, we must observe that both the HX component and the condenser/evaporator component are very simple (no need of expensive pressure-resistant containers, no demisters, etc.). One of the main cost is aluminum, a fairly expensive metal, but this cost is partly balanced by the fact that the life of the system could be extremely long, thanks to its sturdiness, and that aluminum is recoverable at the end of plant's life.

The value of the "optimal ΔT for heat transfer" for a particular plant can be obtained iteratively by introducing different values of ΔT and comparing the resulting costs once all the other parameters have also been introduced and/or calculated.

As a demonstration exercise we have taken into consideration a plant that proceeds with a desalination from 35 ppt up to 70 ppt, characterized by a heat exchange surface of 6,350 m^2, operating at several concentration steps (Table 2).

At the bottom of Table 2, note how the very high thermal conductivity value obtained thanks to the presence of the fins and to a discontinuous feeding implies that the time interval for an acceptable concentration of the evaporating liquid is very short and that this entails a limit to the ΔT for heat transfer value of about 0.6°C (note: the possibility of disregarding this limit by means of particular discharges in the extrusion profile of the tube will be the subject of a future study/research).

The value of 0.6°C for ΔT for heat exchange is however compatible with the values calculated with various simulations: for a kWh price range of 0.75–2 €/kWh optimal values of ΔT are in fact found in the ΔT interval between 0.4°C and 0.7°C, where the values are lower the higher the cost per kWh and the lower the estimated cost for the plant.

Table 3 shows the foreseeable electrical consumption of the compression calculated for this ΔT interval using an electrical efficiency of 94% and a range between 75% and 85% for the mechanical efficiency.

Table 4 shows calculations of the volume of a HX, as described above, needed to serve the evaporator/condenser without the need for auxiliary contributions of thermal energy. The first part of the table calculates the heat available from compression after deducting the thermal losses with the environment and those not recoverable in HX due to NCG. The second part calculates the minimum value of m$_3$ of HX that are necessary according to the ΔT for heat transfer adopted. Note how this volume increases with the increase of the ΔT for heat transfer in a non-proportional way to the increase in production since, as the efficiency decreases with the increase of the ΔT, the amount of heat/ton made available from compression increases. It is therefore not too expensive to adopt the volume of the HX at the maximum value ΔT for heat transfer considered usable in order to ensure greater margins of flexibility in production.

4.1. Non-condensable gases

A small quantity of NCG is dissolved in the feed water which is released in gaseous state following heating. The purging of these NCG is necessary so that their accumulation does not hinder the condensation of the steam.

The volume of the NCG at 102°C and 1 bar is only approximately 143 L (Table 5), that is, it is very small compared to that of the steam to be condensed, the volumetric ratio is approximately 1/12,000. Nevertheless, since the minimum amount of purge required is the greater the lower the heat transfer driving force applied and since in the case of our study, we are using a very low ΔT for heat transfer, NCGs could still theoretically pose a problem.

In fact, for example, with a heat transfer driving force of only 0.4°C, the % content of NCG which zeros the kinetics is 1.47% and the steam to be purged should be rather more than the non-negligible value of approx. 0.58%.

Fortunately, since the device object of the study facilitates multi-step operations, it is therefore consistent to simply subject these purges to additional specific steps of further compression up to much higher ΔT for heat transfer driving force and so reduce the volume of steam to be purged to values below 0.1% undergoing almost negligible extra energy costs of compression (Table 5).

It should also be considered that the final purge of vapor with NCG can be used to feed an HX to heat a fraction of the feed water in aid of the HX which operates on the liquid phases in counter flow.

Table 1
Theoretical compression energy required to obtain 1 ton of distillate *via* vapor compression at 100°C from 35 ppt saline water in multiple operating steps: thermodynamic energy + energy for ΔT heat transfer as a function of concentration steps and ΔT for heat exchange: kWh/ton

E_{theoret} 100°C = Thermodynamic energy 100°C + heat transfer energy 100°C																		
(A) Theoretical thermodynamic compression energy 100°C: $E_{\text{theoret}} = q_v \times \text{BPE}/T_{\text{ev}}$									(B) Heat transfer compression energy 100°C: $E_{\text{theoret}} = q_v \times \Delta T/T_{\text{ev}}$									
Theoretical energy needed for 1 ton of distillate for each 1°C ΔT needed									2,256 J/g × 1°C × (100°C + 273°C) = 6,048 J/g = 1.68 kWh/ton							kWh/(ton·°C)		1.68
Initial ppt of the step (ppt)	Final ppt of the step (ppt)	Residual fraction of saline solution (g/kg)	Evaporated water in the step (g/kg)	Progressive quantity of evaporated water (g/kg)	BPE at the end of the last step (°C)	Weighted average BPE value in the various steps up to the last step (°C)	Advantage in the average value of the BPE obtained by operating in several steps rather than in a single step (°C)	Theoretical energy required for compression at the final salinity of the step (kWh/ton)	Weighted average of theoretical compression energy required in the steps up to the last step (kWh/ton)	Advantage in the value of compression energy required obtained by operating in several steps rather than in a single step (kWh/ton)	Theoretical compression energy for condensation + heat transfer as a function of concentration and ΔT							
											ΔT	0.4	0.5	0.6	0.7	0.8	0.9	1
											kWh/ton due to ΔT	0.672	0.840	1.008	1.176	1.344	1.512	1.680
											Overall theoretical compression energy demand (kWh/ton)							
35	40	875	125.0	125	0.6007	0.6007	0.000	1.009	1.009	0.000		1.68	1.85	2.02	2.19	2.35	2.52	2.69
40	45	777.8	97.2	222.2	0.6852	0.6377	–0.048	1.151	1.071	–0.080		1.74	1.91	2.08	2.25	2.42	2.58	2.75
45	50	700.0	77.8	300.0	0.7717	0.6724	–0.099	1.296	1.130	–0.167		1.80	1.97	2.14	2.31	2.47	2.64	2.81
50	55	636.4	63.6	363.6	0.8603	0.7053	–0.155	1.445	1.185	–0.260		1.86	2.02	2.19	2.36	2.53	2.70	2.86
55	60	583.3	53.0	416.7	0.951	0.7366	–0.214	1.598	1.237	–0.360		1.91	2.08	2.25	2.41	2.58	2.75	2.92
60	65	538.5	44.9	461.5	1.0437	0.7664	–0.277	1.753	1.288	–0.466		1.96	2.13	2.30	2.46	2.63	2.80	2.97
65	70	500.0	38.5	500.0	1.1386	0.7951	–0.344	1.913	1.336	–0.577		2.01	2.18	2.34	2.51	2.68	2.85	3.02
70	75	466.7	33.3	533.3	1.2355	0.8226	–0.413	2.076	1.382	–0.694		2.05	2.22	2.39	2.56	2.73	2.89	3.06
75	80	437.5	29.2	562.5	1.3345	0.8491	–0.485	2.242	1.427	–0.815		2.10	2.27	2.43	2.60	2.77	2.94	3.11
80	85	411.8	25.7	588.2	1.4356	0.8748	–0.561	2.412	1.470	–0.942		2.14	2.31	2.48	2.65	2.81	2.98	3.15
85	90	388.9	22.9	611.1	1.5387	0.8996	–0.639	2.585	1.511	–1.074		2.18	2.35	2.52	2.69	2.86	3.02	3.19
90	95	368.4	20.5	631.6	1.6439	0.9238	–0.720	2.762	1.552	–1.210		2.22	2.39	2.56	2.73	2.90	3.06	3.23
95	100	350.0	18.4	650.0	1.7513	0.9472	–0.804	2.942	1.591	–1.351		2.26	2.43	2.60	2.77	2.94	3.10	3.27

Table 2
Simulation for a desalination from 35 to 70 ppt with a plant with an aluminum heat exchange surface of 6,350 m^2 as a function of the ΔT for heat transfer

Thermal conductivity of the heat exchange wall with intermittent fluid supply								
Thermal conductivity aluminum	W/m·°C	204.00						
Thermal conductivity water	W/m·°C	0.63			U	1/U		
Thickness of the outer layer of percolating condensed saline water in intermittent mode	mm	0.035			18,000	5.556E-05		
Internal layer "equivalent" thickness of percolating condensed water	mm	0.025			25,200	3.968E-05		
Thickness of the aluminum layer	mm	0.7			291,429	3.431E-06		
			Σ 1/U			9.867E-05		
Resulting thermal conductivity with intermittent feeding				W/m^2·°C		***10,135***		
Distillate production per ΔT as a function of driving force for heat transfer over boiling temperature								
Latent heat of evaporation (Table 1)	W/L							627
m^2 of the plant	m^2	6,350.0	6,350.0	6,350.0	6,350.0	6,350.0	6,350.0	6,350.0
ΔT for heat transfer over boiling point temperature	ΔT °C	0.4	0.5	0.6	0.7	0.8	0.9	1.0
Hourly production of distilled H_2O/m^2	L/m^2·h	6.47	8.08	9.70	11.31	12.93	14.55	16.16
Hourly production of distilled H_2O of plant	m^3/h	41.1	51.3	61.6	71.8	82.1	92.4	102.6
Daily production of distilled H_2O of plant	m^3/d	985	1,232	1,478	1,724	1,971	2,217	2,463
Thickness of the percolated film that evaporates every second and seconds available before a given % increase in salt concentration								
Water thickness in the outer film after stopping the brine supply	mm	0.035	0.035	0.035	0.035	0.035	0.035	0.035
Percolated water thickness that evaporates in 1 h	mm	6.47	8.08	9.70	11.31	12.93	14.55	16.16
Percolated water thickness that evaporates every second	mm	1.80E-03	2.25E-03	2.69E-03	3.14E-03	3.59E-03	4.04E-03	4.49E-03
Percentage of increase in the salt concentration of the film that considered acceptable	%	20%	20%	20%	20%	20%	20%	20%
Seconds needed to reach this % increase in salt concentration	s	3.90	3.12	2.60	2.23	1.95	1.73	1.56

Table 3
Energy required for compression as a function of ΔT for heat transfer and compressor efficiency: kWh·elect/ton

ΔT driving force (°C)		0.4			0.5			0.6	
Average BPE at 100°C for a multiple steps 35 to 70 ppt desalination (°C)		0.8			0.8			0.8	
Operative ΔT		1.2			1.3			1.4	
100°C $E_{\text{theoret}} = q_v \times \text{BPE}/T_{\text{ev}}$									
q_v 100°C (J/g)		2,256			2,256			2,256	
T_{ev} (°K)		373			373			373	
1 J/g = 0.277778 (kWh·mech/ton)		0.277778			0.277778			0.277778	
E_{theoret} (kWh·mech/ton)		2.02			2.18			2.35	
compressor efficiency	75%	80%	85%	75%	80%	85%	75%	80%	85%
kWh·mech/ton	2.69	2.52	2.37	2.91	2.73	2.57	3.14	2.94	2.77
Electric efficiency	94%	94%	94%	94%	94%	94%	94%	94%	94%
kWh·elect/ton	2.86	2.68	2.52	3.10	2.90	2.73	3.34	3.13	2.94

Table 4
Theoretical minimum m^2 and m^3 of heat exchanger to combine with a 6,350 m^2 plant as a function of ΔT for heat transfer and a 35 to 70 ppt concentration, with thermal conductivity of heat exchanger surface of 10,135 W/m·°C as calculated in Table 2

(1) Theoretical maximum ΔT available for heat exchanger in the counter-flow heat exchanger							
ΔT for heat transfer over boiling point temperature (°C)	0.4	0.5	0.6	0.7	0.8	0.9	1.0
Heat from mechanical compression available (80% efficiency: Table 3) (kWh·mech/ton)	2.52	2.73	2.94	3.15	3.36	3.57	3.78
Thermal energy lost with NCG purge (kWh/ton)				0.21			
Thermal energy lost with for thermal dispersion (kWh/ton)				0.24			
kWh thermal energy available for HX/ton of distilled water (kWh/ton)	2.07	2.28	2.49	2.70	2.91	3.12	3.33
Tons of source water to be treated/tons of distilled water				2.00			
Maximum ΔT available to heat exchanger to operate (°C)	0.89	0.98	1.07	1.16	1.25	1.34	1.43
(2) Theoretical minimum m^2 and m^3 of heat exchanger							
ΔT for heat transfer over boiling point temperature (°C)	0.4	0.5	0.6	0.7	0.8	0.9	1.0
Maximum ΔT transfer available to heat exchanger to operate (°C)	0.89	0.98	1.07	1.16	1.25	1.34	1.43
Daily production of distilled H_2O of plant (Table 2): m^3/d·plant	985	1,232	1,478	1,724	1,971	2,217	2,463
ΔT °C (from 15°C to 100°C)				85			
Heat exchanger heat capacity (kWh/m^3·°C)				865			
Heat exchanged/h by 1 m^3 heat exchanger at maximum ΔT available (kWh/m^3)	771	849	927	1,005	1,083	1,161	1,239
Minimum m^3 of heat exchanger needed	10.5	12.0	13.1	14.1	15.0	15.7	16.4
Minimum m^2 of surface heat exchanger needed (225.1 m^2/m^3)	2,370	2,690	2,956	3,181	3,374	3,540	3,685
Minimum n° of blocks 1.6 m × 1 m × 1 m heat exchanger needed	6.19	7.03	7.73	8.31	8.82	9.25	9.63
m^3 of heat exchanger per ton of hourly distilled water production	0.26	0.23	0.21	0.20	0.18	0.17	0.16

4.2. $CaCO_3$ and $CaSO_4$ scaling

One of the problems common to thermal desalination processes is $CaCO_3$ and $CaSO_4$ scaling. The problem is caused not only by the increase in concentration that occurs in the desalination process, but also by the fact that their solubility decreases as the temperature increases, and that is the case at 100°C.

Literature reports a long series of treatments to deal with this problem: anti-scalants, treatments with acids, nano-filtration pretreatment, etc. [4,5].

With reference to the technology covered by this study, it should be noted that some of its peculiarities have possible positive effects with respect to this problem and could be the subject of particular attention if the possibility of proceeding to an experimental phase arises.

In this case we would deem it appropriate to experiment with a solution to address scaling that we have not been able to find in literature. Considering that the activation energy which is necessary for the formation of crystals on surfaces not containing already deposited salts is quite greater than that which can be supplied by the simple saturation concentration; considering that the seawater brought to 100°C has a clearly oversaturated concentration of $CaCO_3$ which would therefore allow the formation of new crystals; the solution we intend to experiment is to pass the preheated sea water through layers of very minute calcium crystals so as to cause part of the $CaCO_3$ and $CaSO_4$ to deposit on them and lower the concentration level to a level as close as possible to that of saturation. This process would be repeated in the percolating water collection tanks of percolated water located at the base of each block (Fig. 2A) since evaporation leads to an increase in concentration and therefore increases the saturation level.

The purpose of this operation is to verify whether the competition exerted by the crystals introduced into the collection tanks in capturing the Ca salts present in the seawater, not only thanks to the extremely larger surface they have, but also due to their lower activation energy in capturing the $CaCO_3$/$CaSO_4$, causes that a sufficient supersaturation is not reached to initiate the formation of crystals on the metal surfaces and in any case make that process much more limited/slower (probably made up of a smaller number of crystals which tend to get bigger and therefore more fragile and easily removable).

Similarly, in consideration of the compatibility of our process with the presence of small crystals and/or silt suspended in the feed, it would be interesting to observe the effect of favoring the preferential precipitation precisely in suspension of the calcium salts in the feed, thanks to the introduction in suspension of Ca microcrystals and/or other chemical elements.

With reference to the possibility of $CaCO_3$/$CaSO_4$ scaling we point out how the presence of vertical walls of the evaporator surmounted by the fluid supply allows intense sprays to be carried out at intervals which can carry out a beneficial action.

A further aspect to underline is the fact that the structure envisaged by our study favors, thanks to its modular

Table 5
Non-condensable gases

Purge values using the total volumes of NCG present in the feed water (including CO_2, that is, 72.3% of the total; https://www.steamtablesonline.com/steam97web.aspx?lang=it)												
Input: distillate production (L)	1,000											
Input: feed/distillate concentration factor	2											
Saline water fed (L)	2,000											
Volume of aerobic gas present in saline water °C and 1 bar (mL/L) (http://www.seafriends.org.nz/oceano/seawater.htm#gases)	55											
Percentage of NCG recovered in the post-heat exchanger feed tank (worst case)	0%											
Volume of aerobic gas present in the feed at 102°C and 1 bar (L)	143.2											
Volume of steam processed: d = 0.586 kg/m^3 approx. at T = 102° (https://www.steamtablesonline.com/steam97web.aspx?lang=it) (m^3)	1,706.5											
Volumetric ratio between processed steam and non-condensable gases	11,914											
NCG/steam ratio (%)	0.00839%											
Input: ΔT for heat exchange applied (°C)	0.4	0.5	0.6	0.8	1.0	1.5	2.0	3.0	4.0	5.0	6.0	7.0
ΔP connected: http://www.endmemo.com/chem/vaporpressurewater.php)) (mbar)	14.7	18.4	22.1	29.5	36.9	55.3	73.7	110.6	147.5	184.4	221.2	258.1
Percentage of NCG which zeros the kinetics (1 atm = 1.01325 bar) (%)	1.46%	1.82%	2.18%	2.91%	3.64%	5.46%	7.28%	10.92%	14.56%	18.20%	21.83%	25.47%
Minimum volume of steam to be purged (litres of NCG/% of NCG compatible) (L)	9,840	7,872	6,560	4,920	3,936	2,624	1,968	1,312	984	787	656	562
Equivalent in liters of water of the steam that goes into the purge with reference to 1 t of distillate (L)	5.77	4.61	3.84	2.88	2.31	1.54	1.15	0.77	0.58	0.46	0.38	0.33
Minimum percentage of steam that must be purged together with non-condensable gases (%)	0.577%	0.461%	0.384%	0.288%	0.231%	0.154%	0.115%	0.077%	0.058%	0.046%	0.038%	0.033%
Thermal kWh discharged with purging/t of distillate (627 kWh/ton for condensation + 87°C for thermal delta/,860421 for conv. factor kcal/kw) (kWh/ton)	4.20	3.36	2.80	2.10	1.68	1.12	0.84	0.56	0.42	0.34	0.28	0.24
Same expressed (kcal/t)	3,613	2,890	2,408	1,806	1,445	963	723	482	361	289	241	206

structure in blocks which are easily removable from the main container, their periodic extraction, thus being able to proceed with washing, preferably with the distilled water produced, favoring thus also a recovery of the calcium salts, with much greater recovery if the washing also involves the underlying collection tanks with the bed of calcium salts.

This also applies with reference to the HX if it is modular. We point out that it is also very simple to reverse HX counterflows according to a pre-established timing. In this case it would be possible to observe the possibility that the distilled water with the possible modest addition of, for example, some chemical product can avoid/clean the encrustations forming.

5. Conclusion

Desalination technologies are numerous and each of them has its own advantages and problems. In our opinion the MVC variant developed by this study solves the electric energy consumption problems to an excellent extent and to a large extent those of the plant costs. Compared to other technologies that use exclusively electric energy, MVC offers high quality and pure water, considerable savings in terms of feed treatment (it does not fear problems such as silt, organic biological and inorganic fouling, particulate fouling, algal bloom events, does not require continuous quality controls or many consumables [5] and has a long duration); to its detriment it requires a heat supply for starting the plant and therefore is not suitable for continuous switching on and off, tackles delicate problems due to calcium salts scaling and corrosion which operating at 100°C are more consistent.

We trust that this study will lead to a re-evaluation of the MVC process and pave the way for renewed research that will further improve GMVC efficiency and its economic attractiveness.

Appendix

Assuming a mechanical efficiency of 75% and an electrical efficiency of 94%, the optimal value of electrical energy required for a desalination from 35 to 70 ppt obtained in the study is approximately 3.0 kWh/ton when the cost of electricity, respectively 0.1 €/kWh. A typical optimal unit made of 6,350 m^2 evaporation surface area +3,000 m^2 HX preheating area with the respective heat transfer coefficients of 10.1 and 3.5 $kW/m^2\cdot°K$ will produce 1,000 ton/d of desalted water with a ΔT for heat transfer driving force for evaporation–condensation of 0.4°C and 1°C for preheating heat transfer driving force. The estimated specific investment in evaporation area heat exchange materials/components is of about $160,000, the one in preheating HX materials is of about $60,000. The optimal ΔT value for a heat transfer of 0.4°C is calculated for the assumed practical data: electricity price of 0.1 $/kWh, 8,000 h·operation/y, 30 y of plant life time, 2% annual interest rate over inflation rate with a conservative capital recovery rate of the installed evaporator and HX of $36,000/y.

References

[1] M. Vismara, Evolution of a green mechanical vapor condensation desalination system, Desal. Water Treat., 228 (2021) 14–20.

[2] M. Vismara, N. Mazzetti, R. Mereu, Computational fluid dynamics calculations of high efficiency heat exchangers operating in laminar motion consisting of extruded plastic profiles with inserts, Desal. Water Treat., 293 (2023) 43–48.

[3] H.T. El-Dessouky, H.M. Ettouney, Chapter 10 – Economic Analysis of Desalination Processes, H.T. El-Dessouky, H.M. Ettouney, Eds., Fundamentals of Salt Water Desalination, Elsevier Science, 2002, pp. 503–524, doi: 10.1016/B978-044450810-2/50012-9.

[4] M.A. Farahat, H.E.S. Fath, I.I. El-Sharkawy, S. Ookawara, M. Ahmed, Energy/exergy analysis of solar driven mechanical vapor compression desalination system with nano-filtration pretreatment, Desalination, 509 (2021) 115078, doi: 10.1016/j.desal.2021.115078.

[5] S.G. Salinas-Rodríguez, J.C. Schippers, G.L. Amy, I.S. Kim, M.D. Kennedy, Seawater Reverse Osmosis Desalination: Assessment and Pre-treatment of Fouling and Scaling, IWA Publishing, 2021, doi: 10.2166/9781780409863.